

Article

Photocatalytic Oxidation of Toluene on Fluorine Doped TiO₂/SiO₂ Catalyst Under Simulant Sunlight in a Flat Reactor

Lu Qiu ¹, Yanan Wang ^{2,†}, Hanlinag Li ¹, Gang Cao ², Feng Ouyang ^{1,*} and Rongshu Zhu ^{2,*,†}

¹ Environmental Science and Engineering Research Center, Shenzhen Graduate School, Harbin Institute of Technology, Shenzhen 518055, China; qiulu@hit.edu.cn (L.Q.); lihanliang2012@126.com (H.L.)

² Shenzhen Key Laboratory of Organic Pollution Prevention and Control, Harbin Institute of Technology, Shenzhen 518055, China; wangyn626@foxmail.com; (Y.W.) caog@hotmail.com (G.C.)

* Correspondence: ouyangfh@hit.edu.cn (F.O.); rszhu@hit.edu.cn (R.Z.); Tel.: +86-755-260-33472 (F.O.)

† Co-first author.

Received: 31 October 2018; Accepted: 22 November 2018; Published: 1 December 2018



Abstract: Improving the capacity of TiO₂ semiconductors for visible light response is a key problem for utilization of solar energy in photo-catalytic degradation of organic pollutants. Both catalyst character and reactor conditions are important for the reaction efficiency. The fluorine ion doped TiO₂/SiO₂ catalyst was prepared by sol-gel method using HF solution as fluorine source. The activity test and UV-vis results indicated that this catalyst was superior to TiO₂ P25 in photocatalytic oxidation of gaseous toluene under simulant sunlight irradiation due to the enhancement of visible and ultraviolet light absorbance. GC-MS results indicated that the main intermediates accumulated on active sites included benzoic acid, benzaldehyde, and phenol. A flat interlaid reactor was designed for continuous treatment of the stream with F-TiO₂/SiO₂ film. The results showed that coating the catalyst on the surface of both top and bottom glass substrates, through the knife coating method with an optimal reactor height, attained the highest efficiency. In addition, the presence of water and oxygen enhanced the oxidation of toluene due to the generation of hydroxyl radicals and peroxy radicals, respectively. The toluene oxidation rate increased with the increase in water vapor concentration in the range of 0~60 vol.%.

Keywords: photocatalysis; toluene; oxidation; titanium dioxide; fluorine; reactor

1. Introduction

Volatile organic compounds (VOCs) are major air pollution concerns due to their toxicity or carcinogenicity [1]. Photocatalytic oxidation (PCO) on semiconductor catalysts was proved to be an effective and promising technology to remove VOCs at low concentrations. It is superior to other conventional techniques due to being relatively safe and mild [1,2]. Most organic compounds could be mineralized effectively based on photocatalysts [3]. It was proved that the photo-oxidizing properties of TiO₂ activated by UV plays an important role in the degradation of VOCs [4]. However, TiO₂ is limited in solar energy application due to its low photon utilization efficiency and the need for an ultraviolet excitation source which is less than 10% of the overall solar light [5]. To meet the demands for solar energy utilization, in recent years many efforts have been made to improve visible light response of TiO₂ and restrain its electron-hole pair recombination [6]. Many studies concerned TiO₂ modification by introduction of nonmetals or metal ions into the catalyst. Among these doped nonmetals, a few researchers have reported the improvement of photocatalytic activity by F doped TiO₂ powders [7–15]. Diverse reasons for the improvement of photocatalytic activity by F doping were inferred, including the creation of surface oxygen vacancies [7–10], the formation of OH [11–13],

the increase of Ti^{3+} ions [14], and the enhancement of surface acidity [8,15]. The effects depend on the preparation method. Our previous work has indicated that doping with F anion increased both Lewis and Bronsted acid sites on surface of TiO_2 , and when supported with SiO_2 it significantly improved surface area of the catalyst [15]. It was reported that a catalyst with an acidic surface can easily adsorb polarized organic reactants, and thus promote their photocatalytic decomposition [16–18].

The character of photo-catalytic reactor is another important factor which impacts photocatalytic reaction efficiency. Designing a photocatalytic reactor is significantly challenging due to the dependence of photocatalytic performance on the light absorbance. Photocatalytic reactors for air purification are based on the immobilization of the catalyst onto a substrate. The gas–solid reaction which happened on the catalyst thin film was obviously influenced by surface hydroxyl content, film thickness, and substrates [19–21]. The most widely used gas phase reactors are the flat plate reactor [22–24] and the annular reactor [25–27], which are usually illuminated by UV lamps located at top and center of the reactor, respectively [25,28]. However, in order to simulate sunlight irradiation, the lamp should be located above the reactor, similar to the downward angle of sunlight. As a result, the conditions of the reactor should be designed to fit this irradiation.

In this study, the F doped $\text{TiO}_2/\text{SiO}_2$ catalyst was synthesized by sol–gel method using HF solution as fluorine source. The photocatalytic oxidation of gaseous toluene was studied and the reactions were carried out continuously in a flat interlaid reactor under simulant sunlight. The glass substrates were coated with the F- $\text{TiO}_2/\text{SiO}_2$ catalyst on inner wall of the reactor. In order to improve light efficiency, the effects of the reactor conditions on the toluene oxidation efficiency were tested, including the catalyst coating method, the film location and layers, and the reactor height. The influences of water vapor and oxygen on the photo-catalytic oxidation of toluene were analyzed.

2. Results and Discussion

2.1. Photocatalytic Performance of the F- $\text{TiO}_2/\text{SiO}_2$ Catalyst in Toluene Oxidation

Figure 1a plots the removal of toluene versus irradiation time under simulant sunlight irradiation. The effectiveness of the F- $\text{TiO}_2/\text{SiO}_2$ catalyst was compared with that of TiO_2 P25 (Degussa). The result showed a much higher photocatalytic activity of F- $\text{TiO}_2/\text{SiO}_2$ than TiO_2 P25 for toluene oxidation. The removal efficiency of F- $\text{TiO}_2/\text{SiO}_2$ catalyst reached 91.2% after reacting for 6 min, while the highest removal efficiency of TiO_2 P25 was only 67.4% after reacting for 10 min. Then the degradation activity decreased gradually with the irradiation time. It was inferred that the intermediates were adsorbed on active sites of the catalyst, leading to decrease of available active site numbers of the catalyst.

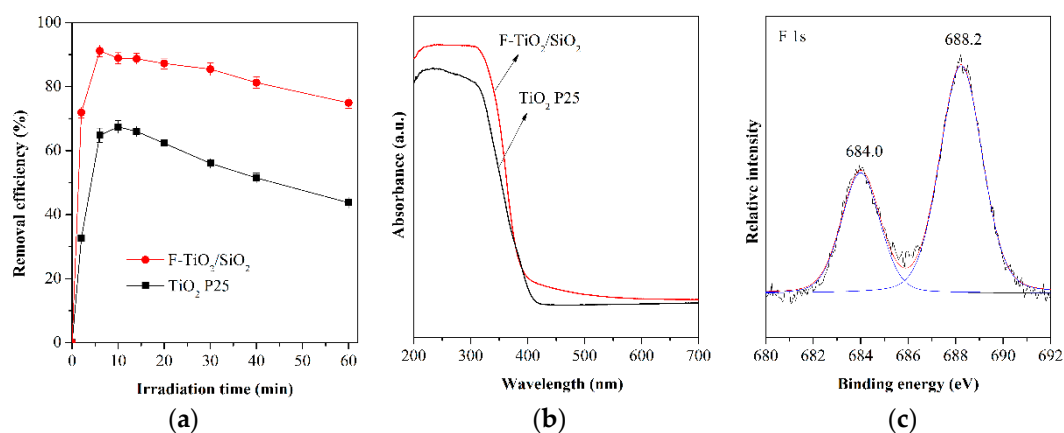


Figure 1. (a) Photocatalytic activities of F- $\text{TiO}_2/\text{SiO}_2$ and TiO_2 P25 catalysts in oxidation of toluene under simulant sunlight, (b) UV-vis diffuse reflectance spectra of F- $\text{TiO}_2/\text{SiO}_2$ and TiO_2 P25. (c) F 1s high-resolution XPS spectra of F- $\text{TiO}_2/\text{SiO}_2$ catalyst.

Figure 1b shows UV-Vis spectra of the F-TiO₂/SiO₂ and TiO₂ P25 catalysts. It can be seen that the F-TiO₂/SiO₂ has a stronger absorption in the ultraviolet region (wavelengths < 400 nm) and visible light region (400~760 nm). This explains the higher photocatalytic activity of F-TiO₂/SiO₂ than TiO₂ P25 under simulant sunlight. In addition, it is deduced that supporting with SiO₂ increases the surface area of the catalyst [15], which is beneficial to the adsorption of the reactants.

Figure 1c shows the XPS spectrum of F 1s in F-TiO₂/SiO₂ catalyst. The spectrum gives two peaks. The higher binding energy one centered at 688.2 eV was attributed to the doped F ions that substituted lattice oxygen of TiO₂ to form the Ti-O-F bond [29,30]. The weaker peak located at 684.0 eV was attributed to surface fluoride species adsorbed on TiO₂ [29]. Based on the XPS result, the atom content of F was 10.4% on surface of F-TiO₂/SiO₂ and about 67.5% of F was presented in the form of Ti-O-F. It indicates most of the F atoms can be incorporated into TiO₂ crystal lattices.

2.2. Optimization of the Catalyst Coating and Reactor Conditions

2.2.1. Effect of Coating Method on Activity of F-TiO₂/SiO₂

The catalyst powders have to be immobilized onto inner surface of the reactor to successively contact with the gaseous pollutants. In this study three coating methods were adopted to immobilize catalyst powders on glass surface. (1) Knife coating method: The catalysts were grinded in a mortar to obtain uniform and fine powders, following by adding deionized water into the mortar with continuous grinding to form stable seriflux. After sticking scotch tapes around the glass-substrate to form a groove, the catalyst seriflux was put into the groove and spread evenly by a glass rod. Then the glass substrates were dried at room temperature for 2 h and subsequently dried at 110 °C for 2 h before being put into the reactor. (2) Spray coating method: Silica solution was used as binder to mix with the catalyst powders with a certain mass ratio, followed by addition of amounts of water and dispersants, sodium hexametaphosphate. This mixed chemical substance was stirred by a magnetic stirrer until stable seriflux formation. The seriflux was then sprayed on the surface of the glass substrates by a spray gun and dried naturally. (3) Sol-gel method: the precursor solution of the catalyst was prepared through the sol-gel method to form sol, which was coated on the surface of the glasses through its adhesive force. Then the glasses were dried at room temperature and subsequently dried in the furnace at 450 °C for 2 h. These coating methods were evaluated through activity for toluene oxidation efficiency and mass loss ratio. The results are shown in Figure 2. The mass loss ratio was defined as Equation (1):

$$\text{mass loss ratio} = (m_0 - m_t) / m_0 \times 100\% \quad (1)$$

where m_0 (mg) is the catalyst quality before coating and m_t (mg) is the catalyst quality after coating and reaction for 1 h.

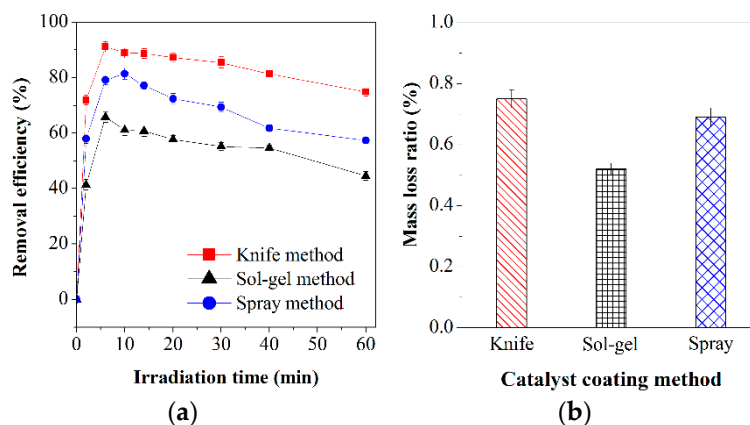


Figure 2. Influence of catalyst coating method on (a) photocatalytic oxidation efficiency of toluene, (b) Mass loss ratio of the catalyst.

From Figure 2, it sees that the order of the mass loss ratio of these coating methods is: sol-gel method (0.52%) < spray method (0.69%) < knife coating method (0.75%), while the order of toluene removal efficiency is: knife coating method > sol-gel method > spray method. The results showed that all of the coating methods provided strong adhesive force of the F-TiO₂/SiO₂ catalyst film on the glass surface, while the knife coating method had the obvious highest removal efficiency of 91.2% for toluene degradation. In addition, it should be considered that the spray coating method needs more catalysts in the process of seriflux preparation than the other loading methods and has a trouble subsequent cleaning work, while the sol-gel loading method needs strict technological conditions in process of precursor preparation, and the catalyst film is easily to chap after calcination in high temperature. The advantages of the knife coating method include the easy operation conditions to form catalyst film, the strong adhesive force between the serous film and the glass substrate, and the good Nano state of the catalyst powders while fully grinded. As a result, the knife coating method was selected to immobilize the catalyst powders on surface of the glass substrate to form a thin film.

2.2.2. Effect of Coating Location and Layers on Activity of F-TiO₂/SiO₂

In order to improve light adsorption efficiency of the catalyst film, different catalyst film locations and layers were investigated, including coating on top glass, bottom glass, and both of the two glasses on the inside of the reactor with the same catalyst dosage (39 mg). The activity test results are shown in Figure 3. It can be seen that coating two glasses has the highest removal efficiency of 91.2% and the highest stability with reaction time, while coating on top glass with the removal efficiency of 89.5% and coating on bottom glass with the removal efficiency of 78.7%. The reason is that on the condition of same catalyst dosage, coating on the top glass could obtain stronger light illumination intensity than coating on the bottom glass, leading to higher removal efficiency of the former. Coating both top and bottom glasses could provide more active sites to toluene molecules adsorption due to the double contact area. However, the light irradiation intensity on bottom glass was insufficient due to absorbance of most light by the top coating catalyst. This was the reason that the difference in toluene oxidation rate between the two glass coatings and the top glass coating was not distinct. As a result, coating on both top and bottom glasses is the optimal pattern for sunlight utilization and is beneficial to photo-catalytic reaction.

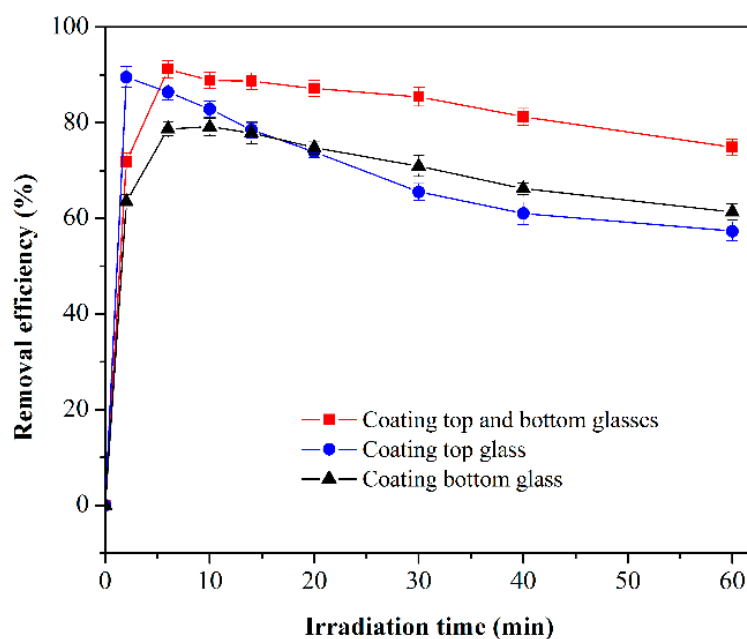


Figure 3. Influence of coating layer and location on photo-catalytic oxidation efficiency of toluene in the flat interlaid reactor.

2.2.3. Effect of Reactor Height on Activity of F-TiO₂/SiO₂

It is significant to optimize the height of the reactor since it effects residence time of the reactor and contact efficiency between the gas molecules and the catalyst film. Figure 4 shows the effect of the reactor height on toluene removal efficiency. It can be seen that in the reactor with 2 mm height, the highest removal efficiency reached 94.1%, higher than the removal efficiency in the reactors with height of 4, 8, and 20 mm. However, the reactor with 4 mm height maintained highest removal efficiency after reacting for 20 min, indicating higher resistance of the catalyst in this reactor. It was deduced that the reaction efficiency was depended on probability of the collision between gaseous toluene molecules and the catalyst films, while here collision probability depended on the contact area, reactor height, and resistance time. Under the same gas flow rate, the smaller reactor height means shorter resistance time, leading to shorter contact time for the toluene molecules and the catalyst film. However, the smaller reactor height benefits the efficient colliding contacts between the toluene molecules and the catalyst active sites. This leads to the highest removal efficiency of the catalyst during the initial time. After reaction for a few minutes, the short resistance time leads to more accumulation of intermediates on catalyst surface, restraining the adsorption of toluene molecules and photocatalytic reactions during later time. Although the reactor with a height of 20 mm had the highest residence time, it was difficult to adequately make contact between the toluene molecules and the catalyst film through molecular diffusion. Therefore, the total collision probability between toluene and catalyst active sites was decreased. There was an optimum reactor height to achieve maximum efficiency between residence time and cross-sectional area of the reactor. Based on the above analysis, the reactor with height of 4 mm was selected.

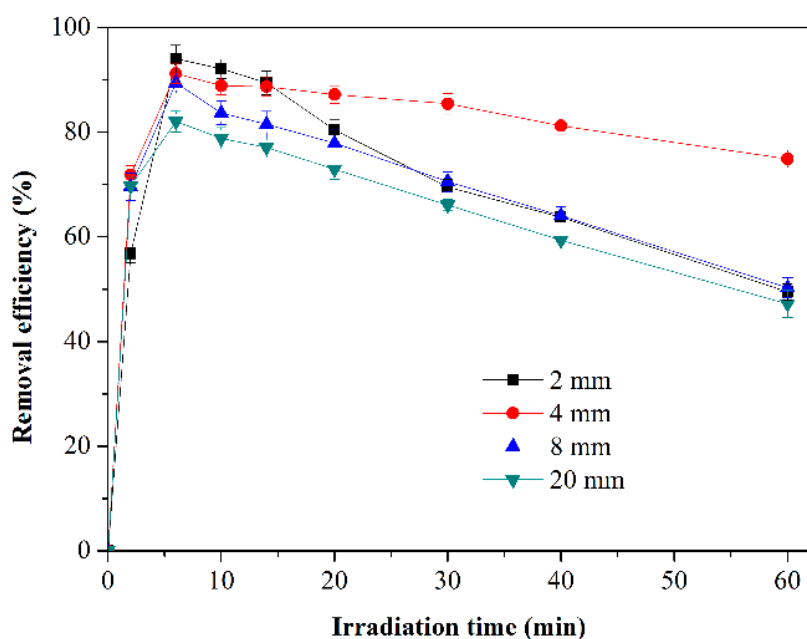


Figure 4. Influence of reactor height on photocatalytic oxidation efficiency of toluene.

2.3. Effect of Initial Toluene Concentration on Toluene Photodegradation

Figure 5 shows the influence of initial toluene concentration on its removal efficiency. The results displayed that the removal efficiency decreased with increase of the initial concentration in the range of 10~50 ppm. The reason is that the photo-catalytic oxidation largely relies on numbers of hydroxyl radicals and active sites on surface of the catalyst. However, both of them are constant quantitatively [31].

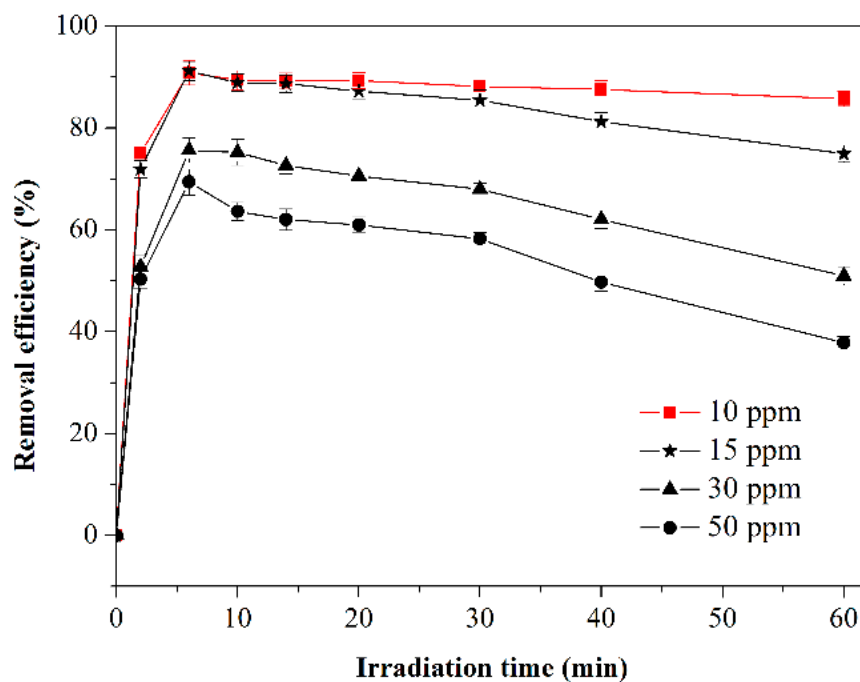
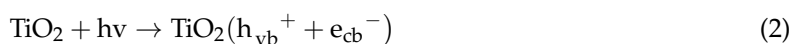


Figure 5. Influence of toluene concentration on photocatalytic oxidation of toluene.

2.4. Effect of Water Vapor on Toluene Photodegradation

Water vapor in gas phase plays an encouraging or suppressive role in photo-catalytic degradation of gas organics. The influence depends on the type of the contaminant and the concentration of water vapor [32]. To investigate the influence of water vapor on toluene oxidation over the F-TiO₂/SiO₂ catalyst, the removal efficiency of toluene was tested under different water vapor concentrations ranging from 0% to 80 vol.%. The results in Figure 6 showed that the catalytic activity for toluene oxidation was increased with the water concentration increased to 60 vol.%, whereas above 60 vol.% concentration the removal efficiency was decreased for about 10%. It is known that the hydroxyl radical on surface of catalyst is essential for photo-catalytic oxidation of organic pollutants as oxidative. In gas–solid heterogeneous reactions, the hydroxyl radicals on surface of the catalyst were consumed quickly without supplement, leading to the decrease of the catalytic activity with times. A certain amount of H₂O could be adsorbed on the catalyst and dissociated to hydroxyl ions, which behaved as a hole trap to generate adsorbed hydroxyl radicals, the reaction are shown in Equations (2)–(4) [33]. This is the reason that water vapor accelerates the toluene oxidation. However, the competitive adsorption of H₂O molecules with the polar toluene molecules on the active sites would reduce the bonds of toluene with catalytic active sites [33,34]. This suppressed the oxidation rate of toluene at high water content [2]. The effect of the water vapor on oxidation activity is the result of competition between positive effect of hydroxyl radical generation and negative effect of competitive adsorption of water and pollutants molecules. For the F-TiO₂/SiO₂ catalyst, the optimum water concentration is 60 vol.%.



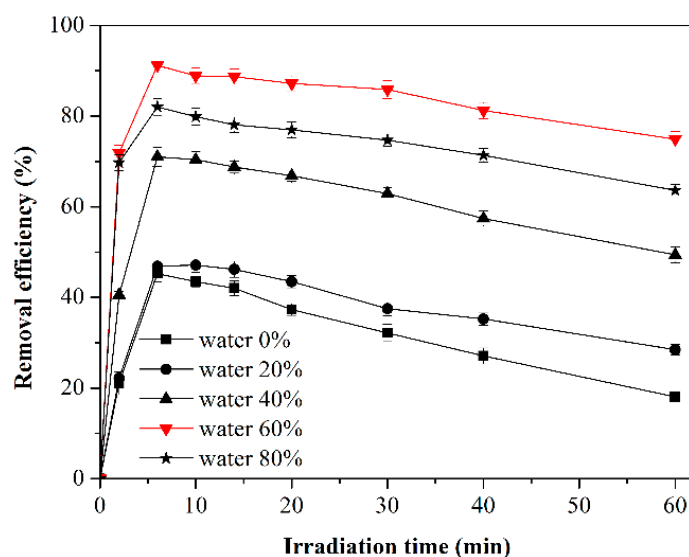


Figure 6. Influence of water vapor concentration on photocatalytic oxidation of toluene.

2.5. Effect of O_2 on Toluene Photodegradation

The influence of oxygen on toluene oxidation over F-TiO₂/SiO₂ thin film was tested by comparing the reaction efficiencies under air and nitrogen atmosphere. The result in Figure 7 revealed that the removal efficiency in air atmosphere was higher than that in nitrogen atmosphere. The highest removal efficiency in air condition was 91.2% after irradiation for 6 min, while the highest removal efficiency in nitrogen atmosphere was 74.3%, indicating the positive effect of oxygen on toluene oxidation. The oxygen could trap the photo-induced electrons to generate peroxy radicals, which retard recombination of the photo-generated electron hole pairs [34]. The peroxy radical could react with water molecule to generate hydroxyl radical, which promotes the photocatalytic degradation of toluene. The reaction pathways are displayed as Equations (5) and (6) [34].

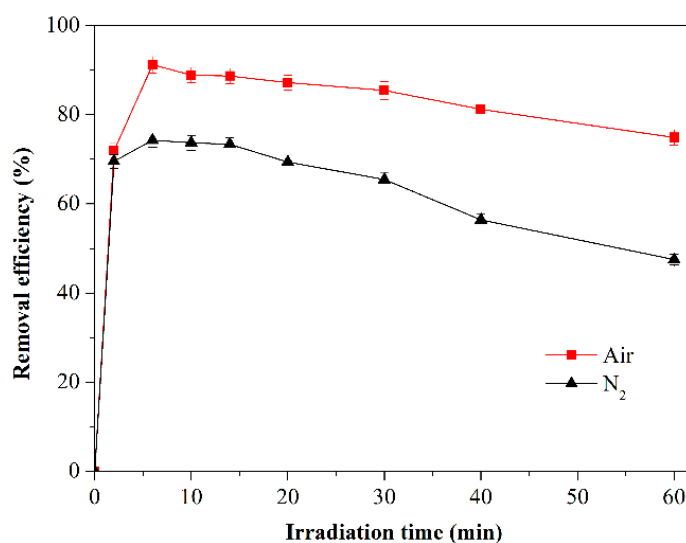
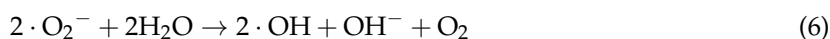


Figure 7. Influence of oxygen on photocatalytic oxidation of toluene.

2.6. Catalyst Deactivation

The catalytic activity decreased with irradiation time and the catalyst thin film turned from white to pale yellow gradually. This was mainly attributed to an accumulation of partially oxidated intermediates on the active sites of the catalyst [2]. In order to learn the species of the intermediates on the F-TiO₂/SiO₂ surface, the deactivated catalyst which used for 2 h were analyzed by GC-MS method, the results are shown in Figure 8. Based on the results, it is known that the main intermediates were benzoic acid, benzaldehyde, and phenol. This indicated highly stable aromatic ring of toluene molecules under simulant sunlight. Luo and Ollis [35] detected only benzoic acid on anatase TiO₂, while more literatures reported benzaldehyde, benzoic acid, and benzyl alcohol are three initial by-products accumulated on TiO₂ surface for toluene photooxidation [2,36–38]. The formation pathway of these intermediates are speculated and depicted in Figure 9. Benzaldehyde and benzoic acid were generated through the benzyl radical, which came from the hydrogen abstraction of the methyl groups [39] and was then attacked by oxygen molecules. In addition, phenol comes from benzoic acid, an OH radical was added to the toluene ring [40]. The final products CO₂ and H₂O were formed while the aromatic ring of toluene or these intermediates were attacked by OH radical addition.

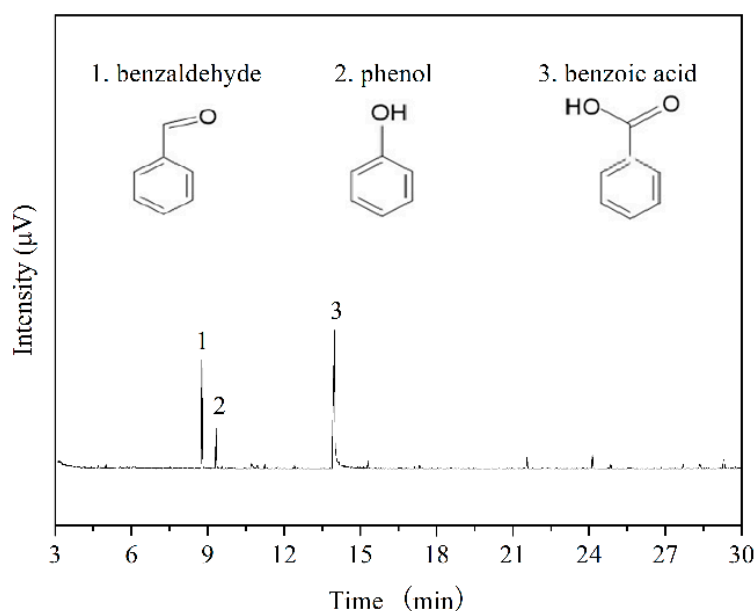


Figure 8. Total chromatogram of intermediates from deactivated F-TiO₂/SiO₂ catalyst detected by GC-MS.

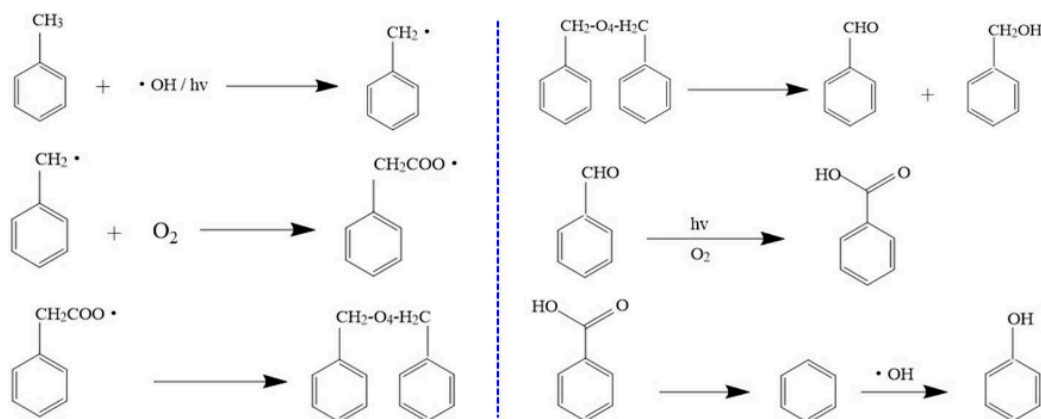


Figure 9. Possible generation pathways of intermediates in the process of photocatalytic oxidation of toluene.

3. Materials and Methods

3.1. Catalyst Preparation

The F-TiO₂/SiO₂ catalyst was prepared by the sol–gel method. All chemicals were analytical grade. Tetrabutyl titanate (Ti(OC₄H₉)₄) was used as a starting material and hydrofluoric acid as a fluorine source. Solution A was formed with a mixture of anhydrous alcohol, acetic acid, deionized water, and hydrofluoric acid solution, which was stirred at room temperature for 20 min. Tetrabutyl titanate was dissolved into anhydrous alcohol to form solution B, while the HF/Ti molar ratio was 1.1. Subsequently, solution A was added dropwise into solution B under vigorous stirring and then the reactor was sealed with cling film. The stirring was lasted for 2–3 h to get homogeneous transparent sol, then the cling film was removed. The silica gel of 100–200 mesh was added into the sol with agitation for 1 h, while the amount of TiO₂ content was 36 wt.%. After aging at room temperature for 10 h, the sol transformed to gel and then was dried at 80 °C for 12 h. The solid was crushed and calcined at 450 °C in air for 2 h.

3.2. Catalyst Evaluation

The photocatalytic degradation processes under simulant sunlight were carried out in a continuous testing system, which consists of a continuous flow reactor, a gas feed system, and an analytical system, shown as Figure 10. The flat interlayer photo-reactor consisted of two stainless steel frames and two glass substrates. The glass substrates (with length of 60 mm, width of 60 mm, and thickness of 1 mm) were coated with catalyst powders and fixed on grooves of the frames, performing as the top and bottom wall of the reaction room. A xenon short arc lamp (350 W, ShenZhen AnHongDa Opto Technology Co., Ltd., Shenzhen, China) with the similar characteristic spectrum with sun light was levelly put above the reactor as an external light source. The lamp was parallel to the gas flow orientation. The distance from the surface of the lamp to top plate of the reactor was 3 mm. The light intensity at surface of the top glass was 26 mW·cm⁻². The irradiated surface of the glass substrate was 50 mm × 50 mm, fully coated catalyst film, while the height of this reactor was controlled by thickness of the groove, shown as Figure 10.

Before coating F-TiO₂/SiO₂ catalyst onto internal glass surface of the reactor, the glasses have to be cleaned carefully to avoid inhomogeneity of the catalyst film. The cleaning process was: (1) Washing the glass with water, following by immersing in NaOH solution to remove oil contaminations. (2) The glass was washed by water again and then immersed in dilute nitric acid with ultrasonic treatment for 30 min to clean away adsorbed metal ions. (3) Washing with water again and immersing in detergent. (4) Washing again and immersing in deionized water with ultrasonic treatment for 10 min, following by drying in the oven at 100 °C.

The simulated reaction gas was supplied from compressed gas cylinders, including standard toluene gas (60 ppm with N₂ as a diluent gas) and dry air (20 vol.% O₂, 80 vol.% N₂). The total flow rate was 80 mL/min, while the initial toluene concentration was 15 ppm and the residence time was 7 s. The flow rates of these gases were measured with mass flow controllers. Water vapor was introduced into the reactor by bubbling the dry air through a water vapor saturator. The water vapor concentration was adjusted by the flow rate of the dry air and the temperature of the water bath. Most experiments were performed at a water concentration of 60 vol.%. The toluene concentrations in the gas flow was analyzed by a gas chromatograph (Model HP 6890, Hewlett–Packard, PaloAlto, CA, USA) equipped with a FID detector. After introduced the mixed gas into the reactor in the dark to reach adsorption saturation, the lamp was turn on to carry out the photo-catalytic reaction. The toluene removal efficiency *R* was calculated by Equation (7):

$$R = (C_0 - C_t) / C_0 \times 100\%, \quad (7)$$

where C_0 and C_t (mg L^{-1}) are concentrations of toluene in adsorption saturation and after light irradiation for minutes, respectively.

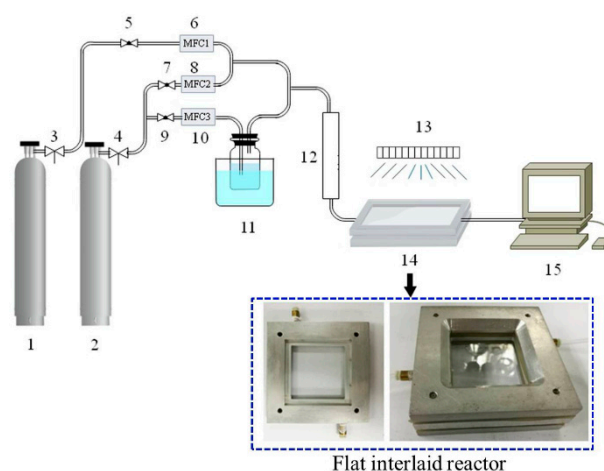


Figure 10. Schematic diagram of the experimental setup for the photolytic oxidation of toluene under simulant sunlight. 1. Toluene gas cylinder; 2. Dry air cylinder; 3, 4. Pressure regulator; 5, 7, 9. Ball valve; 6, 8, 10. Mass flow controller; 11. Water vapor saturator; 12. Gas mixture tube; 13. Xenon lamp; 14. Photo-catalytic reactor; 15. Gas chromatograph.

3.3. GC-MS

Adsorbed intermediates were extracted from the deactivated catalyst by methylene dichloride and ultrasonication. The supernatant was filtered through a $0.2 \mu\text{m}$ filter, followed by rotary evaporation for solute enrichment. Subsequently, the concentrated liquid was filtered through a $0.45 \mu\text{m}$ polytetrafluoroethylene filter. Qualitative analysis of the filtrate was carried on a chromatography-mass (GC-MS) spectrometer (Agilent 5977B GC/MSD, PaloAlto, CA, USA).

4. Conclusions

The F-TiO₂/SiO₂ catalyst exhibited significant higher photocatalytic activity than TiO₂ P25 in gaseous toluene oxidation under simulant sunlight due to its improvement of light absorbance ranges from visible light region to ultraviolet region. A flat interlaid photo-reactor was applied in this work for the continuous photocatalytic reaction. Three reaction intermediates, benzyl alcohol, benzaldehyde, and benzoic acid, were identified on the used catalyst by extraction with methanol. The optimal conditions of the coating procedure and the reactor were evaluated to enhance light utilization and catalytic performance. The results indicated that the optimal coating method for catalyst film was coating on the surface of both top and bottom glass substrates through the knife coating method, and the optimal height of the reactor was 4 mm. The oxidation performance decreased with increase of initial toluene concentration ranges from 10~50 ppm due to the limit of active site numbers. Water vapor played an important role in improving photocatalytic oxidation reaction rate. The optimum water concentration was 60 vol.%. The presence of water and oxygen enhanced the photo-oxidation rate of toluene due to the generation of hydroxyl radical and peroxy radical, respectively.

Author Contributions: Methodology, F.O.; L.Q.; formal analysis, G.C.; R.Z.; Investigation, H.L.; resources, F.O.; L.Q.; Data curation, L.Q.; Y.W.; Writing—original draft preparation, L.Q.; Y.W.; writing—review and editing, F.O.; H.L.; G.C.; R.Z.; Visualization, L.Q., Y.W.

Funding: This research was funded by China Postdoctoral Science Foundation, grant number FD29100012, Foundation Science and Technology innovation Committee of Shenzhen, China, grant number ZDSYS201603301417588 and JCYJ2015731104949798, and National Natural Science Foundation of China, grant number 71371060.

Conflicts of Interest: The authors declare no conflict of interest.

References

1. Korologos, C.A.; Nikolaki, M.D.; Zerva, C.N.; Philippopoulos, C.J.; Pouloupoulos, S.G. Photocatalytic oxidation of benzene, toluene, ethylbenzene and m-xylene in the gas-phase over TiO₂-based catalysts. *J. Photochem. Photobiol. A* **2012**, *244*, 24–31. [[CrossRef](#)]
2. Cao, L.X.; Gao, Z.; Suib, S.L.; Obee, T.N.; Hay, S.O.; Freihaut, J.D. Photocatalytic oxidation of toluene on nanoscale TiO₂ catalysts: Studies of deactivation and regeneration. *J. Catal.* **2000**, *196*, 253–261. [[CrossRef](#)]
3. Boulamanti, A.K.; Philippopoulos, C.J. Photocatalytic degradation of methyl tert-butyl ether in the gas-phase: A kinetic study. *J. Hazard. Mater.* **2008**, *160*, 83–87. [[CrossRef](#)] [[PubMed](#)]
4. Deveau, P.A.; Arzac, F.; Thivel, P.X.; Ferronato, C.; Delpech, F.; Chovelon, J.M.; Kaluzny, P.; Monnet, C. Different methods in TiO₂ photodegradation mechanism studies: Gaseous and TiO₂-adsorbed phases. *J. Hazard. Mater.* **2007**, *144*, 692–697. [[CrossRef](#)] [[PubMed](#)]
5. Sun, S.; Ding, J.J.; Bao, J.; Gao, C.; Qi, Z.M.; Yang, X.Y.; He, B.; Li, C.X. Photocatalytic degradation of gaseous toluene on Fe-TiO₂ under visible light irradiation: A study on the structure, activity and deactivation mechanism. *Appl. Surf. Sci.* **2012**, *258*, 5031–5037. [[CrossRef](#)]
6. Pelaez, M.; Nolan, N.T.; Pillai, S.C.; Seery, M.K.; Falaras, P.; Kontos, A.G.; Dunlop, P.S.M.; Hamilton, J.W.J.; Anthony Byrne, J.; O'Shea, K.; et al. A review on the visible light active titanium dioxide photocatalysts for environmental applications. *Appl. Catal. B* **2012**, *125*, 331–349. [[CrossRef](#)]
7. Li, D.; Haneda, H.; Labhsetwar, N.K.; Hishita, S.; Ohashi, N. Visible-light-driven photocatalysis on fluorine-doped TiO₂ powders by the creation of surface oxygen vacancies. *Chem. Phys. Lett.* **2005**, *401*, 579–584. [[CrossRef](#)]
8. Li, D.; Haneda, H.; Hishita, S.; Ohashi, N.; Labhsetwar, N.K. Fluorine-doped TiO₂ powders prepared by spray pyrolysis and their improved photocatalytic activity for decomposition of gas-phase acetaldehyde. *J. Fluor. Chem.* **2005**, *126*, 69–77. [[CrossRef](#)]
9. Ho, W.; Yu, J.C.; Lee, S. Synthesis of hierarchical nanoporous F-doped TiO₂ spheres with visible light photocatalytic activity. *Chem. Commun.* **2006**, *10*, 1115–1117. [[CrossRef](#)] [[PubMed](#)]
10. Yu, C.L.; Zhou, W.Q.; Yang, K.; Rong, G. Hydrothermal synthesis of hemisphere-like F-doped anatase TiO₂ with visible light photocatalytic activity. *J. Mater. Sci.* **2010**, *45*, 5756–5761. [[CrossRef](#)]
11. Minero, C.; Mariella, G.; Maurino, V.; Pelizzetti, E. Photocatalytic transformation of organic compounds in the presence of inorganic anions. 1. Hydroxyl-mediated and direct electron-transfer reactions of phenol on a titanium dioxide-fluoride system. *Langmuir* **2000**, *16*, 2632–2641. [[CrossRef](#)]
12. Minero, C.; Mariella, G.; Maurino, V.; Vione, D.; Pelizzetti, E. Photocatalytic transformation of organic compounds in the presence of inorganic ions. 2. Competitive reactions of phenol and alcohols on a titanium dioxide-fluoride system. *Langmuir* **2000**, *16*, 8964–8972. [[CrossRef](#)]
13. Vohra, M.S.; Kim, S.; Choi, W. Effects of surface fluorination of TiO₂ on the photocatalytic degradation of tetramethylammonium. *J. Photochem. Photobiol. A* **2003**, *160*, 55–60. [[CrossRef](#)]
14. Yu, J.C.; Yu, J.G.; Ho, W.K.; Jiang, Z.T.; Zhang, L.Z. Effects of F⁻ doping on the photocatalytic activity and microstructures of nanocrystalline TiO₂ powders. *Chem. Mater.* **2002**, *14*, 3808–3816. [[CrossRef](#)]
15. Pang, D.D.; Wang, Y.T.; Ma, X.D.; Ouyang, F. Fluorine promoted and silica supported TiO₂ for photocatalytic decomposition of acrylonitrile under simulant solar light irradiation. *Chem. Eng. J.* **2014**, *258*, 43–50. [[CrossRef](#)]
16. Kwon, Y.T.; Song, K.Y.; Lee, W.I.; Choi, G.J.; Do, Y.R. Photocatalytic behavior of WO₃-loaded TiO₂ in an oxidation reaction. *J. Catal.* **2000**, *191*, 192–199. [[CrossRef](#)]
17. Keller, V.; Bernhardt, P.; Garin, F. Photocatalytic oxidation of butyl acetate in vapor phase on TiO₂, Pt/TiO₂ and WO₃/TiO₂ catalysts. *J. Catal.* **2003**, *215*, 129–138. [[CrossRef](#)]
18. Zhao, D.; Chen, C.; Wang, Y.; Ji, H.; Ma, W.; Zang, L.; Zhao, J. Surface modification of TiO₂ by phosphate: Effect on photocatalytic activity and mechanism implication. *J. Phys. Chem. C* **2008**, *112*, 5993–6001. [[CrossRef](#)]
19. Yu, J.G.; Zhao, X.J.; Du, J.C.; Chen, W.M. Preparation, Microstructure and photocatalytic activity of the porous TiO₂ anatase coating by sol-gel processing. *J. Sol-Gel Sci. Technol.* **2000**, *17*, 163–171. [[CrossRef](#)]
20. Yu, J.G.; Zhao, X.J. Effect of substrates on the photocatalytic activity of nanometer TiO₂ thin films. *Mater. Res. Bull.* **2000**, *35*, 1293–1301. [[CrossRef](#)]

21. Yu, J.G. Photocatalytic activity and characterization of the sol-gel derived Pb-doped TiO₂ thin films. *J. Sol-Gel Sci. Technol.* **2002**, *24*, 39–48. [[CrossRef](#)]
22. Obee, T.N.; Hay, S.O. Effects of moisture and temperature on the photooxidation of ethylene on titania. *Environ. Sci. Technol.* **1997**, *31*, 2034–2038. [[CrossRef](#)]
23. Puddu, V.; Choi, H.; Dionysiou, D.D.; Puma, G.L. TiO₂ photocatalyst for indoor air remediation: Influence of crystallinity, crystal phase, and UV radiation intensity on trichloroethylene degradation. *Appl. Catal. B Environ.* **2010**, *94*, 211–218. [[CrossRef](#)]
24. Salvadó-Estivill, I.; Brucato, A.; Puma, G.L. Two-dimensional modeling of a flatplate photocatalytic reactor for oxidation of indoor air pollutants. *Ind. Eng. Chem. Res.* **2007**, *46*, 7489–7496. [[CrossRef](#)]
25. Blommaerts, N.; Asapu, R.; Claes, N.; Bals, S.; Lenaerts, S.; Verbruggen, S.W. Gas phase photocatalytic spiral reactor for fast and efficient pollutant degradation. *Chem. Eng. J.* **2017**, *316*, 850–856. [[CrossRef](#)]
26. Jović, F.; Kosar, V.; Tomašić, V.; Gomzi, Z. Non-ideal flow in an annular photocatalytic reactor. *Chem. Eng. Res. Des.* **2012**, *90*, 1297–1306. [[CrossRef](#)]
27. Tomašić, V.; Jović, F.; Gomzi, Z. Photocatalytic oxidation of toluene in the gas phase: Modelling an annular photocatalytic reactor. *Catal. Today* **2008**, *137*, 350–356. [[CrossRef](#)]
28. Boyjoo, Y.; Ang, M.; Pareek, V. Light intensity distribution in multi-lamp photocatalytic reactors. *Chem. Eng. Sci.* **2013**, *93*, 11–21. [[CrossRef](#)]
29. Wu, Y.M.; Xing, M.Y.; Tian, B.Z.; Zhang, J.L.; Chen, F. Preparation of nitrogen and fluorine co-doped mesoporous TiO₂ microsphere and photodegradation of acid orange 7 under visible light. *Chem. Eng. J.* **2010**, *162*, 710–717. [[CrossRef](#)]
30. Yang, G.D.; Jiang, Z.; Shi, H.H.; Jones, M.O.; Xiao, T.C.; Edwards, P.P.; Yan, Z.F. Study on the photocatalysis of F-S co-doped TiO₂ prepared using solvothermal method. *Appl. Catal. B Environ.* **2010**, *96*, 458–465. [[CrossRef](#)]
31. Huang, H.; Huang, H.; Lu, Z.; Peng, H.; Ye, X.; Leung, D.Y.C. Enhanced degradation of gaseous benzene under vacuum ultraviolet (VUV) irradiation over TiO₂ modified by transition metals. *Chem. Eng. J.* **2015**, *259*, 534–541. [[CrossRef](#)]
32. Korologos, C.A.; Philippopoulos, C.J.; Pouloupoulos, S.G. The effect of water presence on the photocatalytic oxidation of benzene, toluene, ethylbenzene and m-xylene in the gas-phase. *Atmos. Environ.* **2011**, *45*, 7089–7095. [[CrossRef](#)]
33. Jeong, J.; Sekiguchi, K.; Sakamoto, K. Photochemical and photocatalytic degradation of gaseous toluene using short-wavelength UV irradiation with TiO₂ catalyst: Comparison of three UV sources. *Chemosphere* **2004**, *57*, 663–671. [[CrossRef](#)] [[PubMed](#)]
34. Kim, S.B.; Hwang, H.T.; Hong, S.C. Photocatalytic degradation of volatile organic compounds at the gas–solid interface of a TiO₂ photocatalyst. *Chemosphere* **2002**, *48*, 437–444. [[CrossRef](#)]
35. Luo, Y.; Ollis, D.F. Heterogeneous photocatalytic oxidation of trichloroethylene and toluene mixtures in air: Kinetic promotion and inhibition, time-dependent catalyst activity. *J. Catal.* **1996**, *163*, 1–11. [[CrossRef](#)]
36. D’Hennezel, O.; Pichat, P.; Ollis, D.F. Benzene and toluene gas-phase photocatalytic degradation over H₂O and HCL pretreated TiO₂: By-products and mechanisms. *J. Photochem. Photobiol. A* **1998**, *118*, 197–204. [[CrossRef](#)]
37. Guo, T.; Bai, Z.P.; Wu, C.; Zhu, T. Influence of relative humidity on the photocatalytic oxidation (PCO) of toluene by TiO₂ loaded on activated carbon fibers: PCO rate and intermediates accumulation. *Appl. Catal. B* **2008**, *79*, 171–178. [[CrossRef](#)]
38. Van Durme, J.; Dewulf, J.; Sysmans, W.; Leys, C.; Van Langenhove, H. Abatement and degradation pathways of toluene in indoor air by positive corona discharge. *Chemosphere* **2007**, *68*, 1821–1829. [[CrossRef](#)] [[PubMed](#)]
39. Mo, J.H.; Zhang, Y.P.; Xu, Q.J.; Zhu, Y.F.; Lamson, J.J.; Zhao, R.Y. Determination and risk assessment of by-products resulting from photocatalytic oxidation of toluene. *Appl. Catal. B Environ.* **2009**, *89*, 570–576. [[CrossRef](#)]
40. Frankcombe, T.J.; Smith, S.C. OH-initiated oxidation of toluene. 1. Quantum chemistry investigation of the reaction path. *J. Phys. Chem. A* **2007**, *111*, 3686–3690. [[CrossRef](#)] [[PubMed](#)]

